Catalysis Today 185 (2012) 94–98

Contents lists available at SciVerse ScienceDirect

Catalysis Today

journal homepage: www.elsevier.com/locate/cattod

Structural stability of AgCu bimetallic nanoparticles and their application as a catalyst: A DFT study

Kihyun Shin, Da Hye Kim, Sang Chul Yeo, Hyuck Mo Lee*

Department of Material Science and Engineering, KAIST, 291 Daehak-ro, Yuseong-gu, Daejeon, 305-701, Republic of Korea

ARTICLE INFO

Article history:
Received 1 June 2011
Received in revised form 22 August 2011
Accepted 16 September 2011
Available online 10 October 2011

Keywords:
Oxygen reduction reaction
AgCu bimetallic nanoparticle
Density functional theory
Structural stability

ABSTRACT

Density functional theory (DFT) calculations confirm the structural stability of isomers for 13-atom Ag, Cu, and AgCu nanoparticles. Ag_{13} and Cu_{13} nanoparticles have a different stable structure because of the quantum effect and differences in surface energy. We systematically studied the oxygen reduction reaction (ORR) of Ag_{13}, Cu_{13}, $Ag_{12}Cu_1$ (core–shell) and $Ag_{12}Cu_1$ (alloy) nanoparticles by investigating the adsorption property of O_2 and the transition state calculations of O_2 dissociation, which determine the ORR rate. An Ag alloy with Cu has the high adsorption energy and a low energy barrier. It also exhibits the high structural stability during the reaction.

1. Introduction

The seriousness of problems with energy supplies and environmental pollution is creating greater interest in fuel cells and lithium batteries. Fuel cells produce electricity by electrochemically converting hydrogen and oxygen into water [1]. In fuel cells, noble metals such as Pt are used as a catalyst for the ORR [2–5]. However, the high cost of Pt has sparked a search for a Pt substitute or new ways of reducing the quantity of Pt required. For example, in contrast to Au bulk materials, Au nanoparticles can be used in many selective oxidation reactions [6–18]. Several bimetallic nanoparticles have been recommended for use in a catalytic system [3,19–29].

Our research is focused on intrinsic metal effects. We ignore other effects, such as support. Although such effects are still important [8,30,31], we hope to gain a better understanding of the catalytic reaction on bare nanoparticles by systematically investigating how the alloying procedure or the nanoparticle configuration affects the catalytic activity and structural stability. A clear understanding of the reaction mechanism is essential for validating the catalytic properties of new materials. The ORR can be expressed as follows:

$$1/2O_2 + * \rightarrow O* \quad (R1)$$

$$O* + H^+ + e^- \rightarrow HO* \quad (R2)$$

$$HO* + H^+ + e^- \rightarrow H_2O + * \quad (R3)$$

where * denotes a site on the nanoparticle and the O_2 dissociation reaction (R1) is the rate determining step. We focus on (R1) as a means of validating the catalytic properties. As part of the researches, we selected an AgCu bimetallic nanoparticle as a new catalyst for ORR. ORR activity of the pure Ag or Cu is low than Pd or Pt because O_2 adsorption energy on Ag is too low, while O_2 adsorption energy on Cu is too high [32]. We expect that each property of Ag and Cu affects O_2 adsorption property on an AgCu bimetallic material and leads AgCu bimetallic nanoparticle to have proper adsorption strength and to become a good catalyst for ORR. Moreover, Ag and Cu are much less expensive than Pt or Pd. On 17 August 2011, the metal prices are 40.29 $/troy oz, 0.28 $/troy oz, 1840.80 $/troy oz, 779.65 $/troy oz for Ag, Cu, Pt and Pd, respectively [33]. The structural stability of nanoparticles is a key factor. Many researchers have endeavored to find a stable nanoparticle structure [34–39]. We use DFT calculations to determine the stable structure of Ag_{13}, Cu_{13}, and $Ag_{12}Cu_1$ nanoparticles. Then, we evaluate the O_2 adsorption and the O_2 dissociation on the nanoparticles by DFT calculations.

2. Computational details

We performed GGA-level spin-polarized DFT calculations with the atomic orbital based DMol^3 code for energetically structure stabilities and catalytic properties of Ag, Cu, and AgCu bimetallic nanoparticles. The exchange correlation energy was functionalized with the RPBE functional. The Kohn-Sham equation was expanded in a double numeric quality basis set with polarization functions (DNP). The orbital cutoff range was 5.0 Å. The DFT sem core pseudo potential was used to treat the core electrons of heavy Ag and Cu

* Corresponding author. Tel.: +82 42 350 3334; fax: +82 42 350 3310.
E-mail address: hmlee@kaist.ac.kr (H.M. Lee).

0920-5861/$ – see front matter © 2011 Elsevier B.V. All rights reserved.
doi:10.1016/j.cattod.2011.09.022

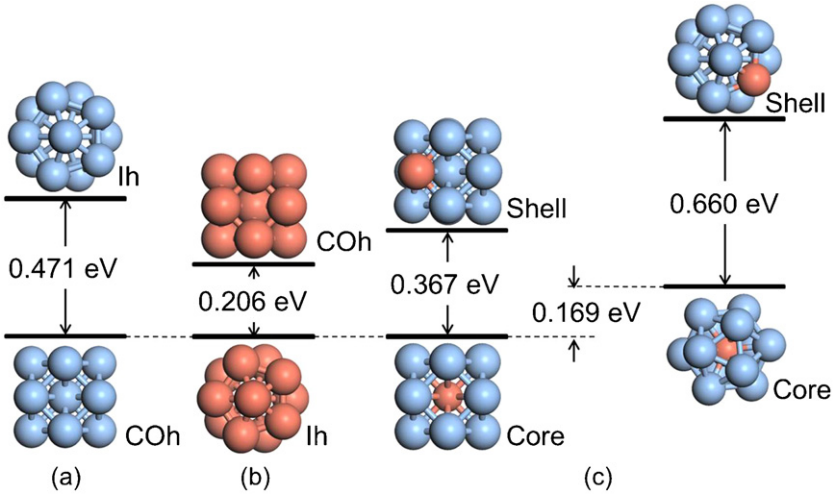

Fig. 1. Energy difference between the COh and Ih structures in (a) Ag_{13}, (b) Cu_{13}, and (c) $Ag_{12}Cu_1$ nanoparticles.

atoms. We used a Fermi smearing method with a window size of 0.002 hartree (Ha) (1 Ha = 27.2114 eV). The energy, force, and displacement convergence criterion were set to 10^{-5} Ha, 0.002 Ha/Å, and 0.005 Å, respectively.

For effective analysis, we simplified the system of the DFT calculations. We prepared Ag_{13}, Cu_{13}, and $Ag_{12}Cu_1$ nanoparticles with two types of structures: a cuboctahedron (COh) and an icosahedron (Ih). These structures are well known as the isomers of a nanoparticle with 13-atom. We considered two configurations of the $Ag_{12}Cu_1$ nanoparticle. The first is a core–shell structure (with copper substituted for an Ag atom in the core): namely, $Ag_{12}Cu_1$ (core–shell). The second is an alloy structure (with copper substituted for an Ag atom in the shell); namely $Ag_{12}Cu_1$ (alloy).

The transition state calculations for the O_2 dissociation reaction were performed with a synchronous transit method, a linear synchronous transit method, and a quadratic synchronous transit method. These methods were combined with a conjugate gradient minimization algorithm for subsequent refinement.

3. Results and discussion

3.1. Structural stability

In Fig. 1, the Ag_{13} and Cu_{13} nanoparticles have different levels of structural stability among the isomers of a 13-atom nanoparticle. In the Ag_{13} nanoparticle, the stability of the COh structure exceeds that of the Ih structure by 0.471 eV; in the Cu_{13} nanoparticle, the stability of the Ih exceeds that of the COh structure by 0.206 eV. The energy difference between the COh and Ih structures in the pure Cu nanoparticle is smaller than the corresponding energy difference in the pure Ag nanoparticle.

The total energy of a nanoparticle consists of internal energy and surface energy. The ratio of the surface to volume increases with smaller particles. Thus, the effect of the surface energy on the total energy of the entire system has become increasingly important. Reducing the surface energy is therefore a significant factor in nano-sized systems that reduce the total energy of nanoparticles.

Although a face centered cubic (FCC) structure is the most stable structure of pure Ag and Cu in bulk materials, another Ih structure with five-fold symmetry has been found in nano-sized systems. A close packed (1 1 1) surface has the lowest surface energy. One way to decrease the surface energy and, ultimately, the total energy is to form an Ih structure that includes all the twenty surfaces of the (1 1 1) surface. In addition, the Ih structure has two types of bond lengths. The bond between a core atom and a shell atom is shorter than the bond between two shell atoms. That is, a nanoparticle of an Ih structure is under compressive stress in the direction of the core–shell. We speculate that the internal energy of an Ih structure is higher than that of a COh structure.

Our DFT calculations for the Cu nanoparticle show that the Ih is more stable than the COh having FCC symmetry. These days, however, many researchers can experimentally control the structure of nanoparticles. If Cu_{13} nanoparticles with COh are synthesized and the catalytic properties are examined, then very weird results may come out. This kind of predictive study can help to avoid unnecessary experimental trials. In this way, we considered both structures. As shown in Fig. 1, the DFT calculations for the Ag_{13} nanoparticle show that the COh is more stable than the Ih structure. The internal energy and surface energy are in a competition to reduce the total energy. For an Ag_{13} nanoparticle with a lower surface energy than that of Cu_{13} nanoparticle, the internal energy can be effective to reduce the total energy. However, the surface energy can be effective to reduce the total energy in the case of a Cu_{13} nanoparticle with a higher surface energy. The surface energy is 1.32 J/m^2 for silver and 1.77 J/m^2 for copper [40].

In the case of the $Ag_{12}Cu_1$ bimetallic nanoparticle, we considered two configurations by the position of the Cu atom: $Ag_{12}Cu_1$ (core–shell) and $Ag_{12}Cu_1$ (alloy). In Fig. 1(c), $Ag_{12}Cu_1$ nanoparticles having the COh and Ih structures have the same stable configuration of a core–shell structure. This configuration is caused by the fact that Cu has a higher surface energy than Ag. As a result, the optimum configuration is to have the Cu atom in the core of the nanoparticle and the Ag atom in the shell of the nanoparticle.

Fig. 1(c) shows that the energy difference between the COh and Ih was 0.169 eV in $Ag_{12}Cu_1$ (core–shell). This value is smaller than the 0.471 eV energy difference found in a pure Ag_{13} nanoparticle or the 0.206 eV found in a pure Cu_{13} nanoparticle. As mentioned, the Ih structure was under some stress. For an Ag_{13} nanoparticle, the bond length is 2.87 Å between the core–shell atoms and 3.03 Å between the shell–shell atoms. The difference in bond length induces stress and strain in the Ih structure of a pure Ag nanoparticle. The Ih structure suffers compressive stress in the core–shell direction and tensile stress in the shell–shell direction. We found that when an Ag atom in the core was replaced with a Cu atom, which has a smaller atomic size, the bimetallic nanoparticle $Ag_{12}Cu_1$ (core–shell) shrinks. The difference in bond length between the core–shell atoms and the shell–shell atoms is reduced. Thus the stress in the Ih structure is reduced by Cu substitution and the structure is stabilized [39].

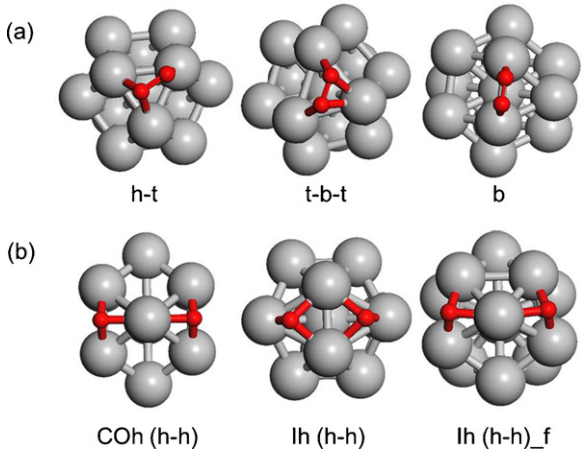

Fig. 2. (a) Configurations of an oxygen molecule adsorption, (b) the adsorption of two oxygen atoms on two hollow sites of the COh and Ih structures of a metal nanoparticle.

In summary, Ag, which has less surface energy than that of Cu, has a stable COh structure. The Ih structure is more stable than COh structure in the Cu_{13} nanoparticle. In the same way, $Ag_{12}Cu_1$ (core–shell) is more stable than $Ag_{12}Cu_1$ (alloy) because Ag and Cu have different levels of surface energy. The substitution of a Cu atom for a core Ag atom alleviates stress and strain in the Ih structure and reduces the energy difference between the COh and the Ih. This energy difference between the two structures is related to renewable catalysts, which are explained in the following section.

3.2. O_2 dissociation on Ag_{13}, Cu_{13}, and $Ag_{12}Cu_1$ nanoparticles

The cathode of a fuel cell undergoes a continual ORR. For an ORR, the O_2 adsorption and the O_2 dissociation processes are essential for determining the rate and activity level of the entire reaction. In other words, the adsorption and dissociation of an oxygen molecule in an ORR must be considered for identification of the catalytic properties of an AgCu nanoparticle. Our investigation of an O_2 dissociation reaction of a 13-atom nanoparticle revealed that an oxygen molecule and two oxygen atoms had strong adsorption sites. Fig. 2(a) shows the configuration of the adsorbed oxygen molecule, and Fig. 2(b) shows the configuration of the two adsorbed oxygen atoms. The oxygen molecule has three optimal adsorption sites: a hollow top (h-t), a top bridge top (t-b-t), and a bridge (b). The molecule adsorbed on the b site of the edge between the two metal atoms is symmetrical but located asymmetrically at the t-b-t site, slightly toward the (1 1 1) surface. The $Ag_{12}Cu_1$ (alloy) nanoparticle has two types of h-t sites. When an oxygen molecule is adsorbed at the h-t site, the Cu substitution can occur at the hollow site (h(Cu)-t) or the top site (h-t(Cu)).

Table 1 lists the adsorption energy, the electron transfer amount, and bond length of O–O at each site and configuration. The oxygen molecule accepts electrons from Ag and Cu metal atoms and the antibonding states of the oxygen molecule are occupied. It weakens the binding energy of the oxygen molecule and consequently lengthens the bond length of the oxygen molecule. Thus it affects the O_2 dissociation. However, to predict a strong adsorption site, we need to analyze other factors such as the structure, the charge flow, the bond length, and the density of states.

Table 1 shows that a threefold h-t site has the strongest adsorption energy on the Ag_{13} nanoparticle. In the case of the Cu_{13} nanoparticle, all the sites have about −1.7 eV of adsorption energy. In the chemisorption of transition metals, the shift of the d-band affects the O_2 adsorption energy [41]. Fig. 3 plots the d-bands of against each composition and configuration. The d-band center of

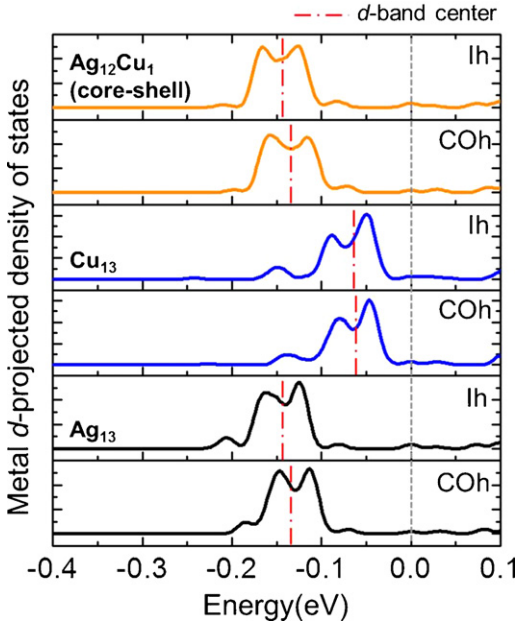

Fig. 3. Metal *d*-projected density of states of each system.

Ag_{13} nanoparticle is much further below the Fermi level than the d-band center of Cu_{13} nanoparticle. O_2 adsorption energy of Cu_{13} nanoparticle is three times higher than that of Ag_{13} nanoparticle. $Ag_{12}Cu_1$ (core–shell), which has Cu as a core atom and only Ag as a shell atom, has similar d-band center of Ag_{13} nanoparticle. Thus there is no significant benefit for the O_2 adsorption on the surface of the nanoparticle. When O_2 is directly bonded to a Cu atom on the surface of an $Ag_{12}Cu_1$ (alloy) nanoparticle, the adsorption energy is two times higher than that of Ag_{13} nanoparticle.

As shown in Fig. 4, O_2 adsorption on a metal nanoparticle induces structural change in Ag_{13} and Cu_{13} nanoparticles. In both cases, the relatively unstable structure becomes stable trough the transformation. That is, the Ih changes to a COh in an Ag_{13} nanoparticle and the COh changes to an Ih in a Cu_{13} nanoparticle. These structural changes are not good for a catalyst because catalytic property is decreased. In some case, nanoparticles were deformed into amorphous structure by adsorbates. Amorphous nanoparticle has very low catalytic activity in our previous study [19]. Thereby structure change is reducing the renewability of the catalyst. In

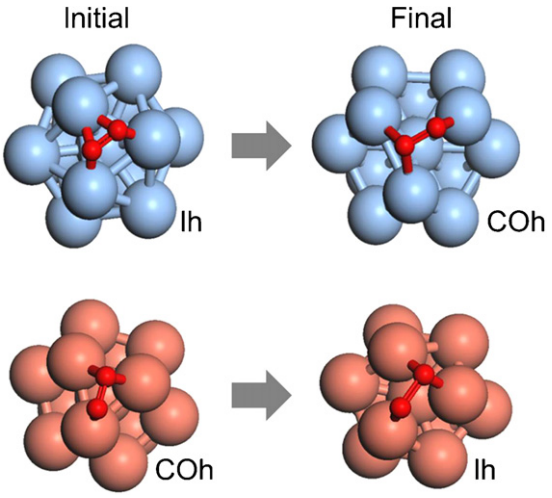

Fig. 4. Structural change for a relatively unstable structure in Ag_{13} (upper) and Cu_{13} (bottom) nanoparticles.

Table 1
The adsorption energy (E_{ad}), the electron transfer amount, and the bond length of O–O (d_{O-O}) for each configuration and adsorption site.

	Structure	Site	E_{ad} (eV)	Mulliken charge of O_2	d_{O-O} (Å)
	COh	h-t	−0.509	−0.308	1.401
		t-b-t	−0.436	−0.340	1.427
Ag_{13}	Ih	h-t	−0.775	−0.314	1.398
		t-b-t		Structure change to COh	
		b	−0.584	−0.261	1.343
	COh	h-t		Structure change to Ih	
		t-b-t	−1.760	−0.341	1.528
Cu_{13}	Ih	h-t	−1.758	−0.326	1.504
		t-b-t	−1.734	−0.334	1.527
		b	−1.741	−0.260	1.409
	COh	h-t	−0.415	−0.314	1.415
		t-b-t	−0.453	−0.331	1.420
$Ag_{12}Cu_1$ (core–shell)	Ih	h-t	−0.652	−0.315	1.403
		t-b-t	−0.577	−0.335	1.429
		b	−0.480	−0.261	1.355
	COh	h-t(Cu)	−0.987	−0.335	1.446
		h(Cu)-t	−0.905	−0.335	1.445
		t-b-t	−0.955	−0.351	1.476
$Ag_{12}Cu_1$ (alloy)	Ih	h-t(Cu)	−1.254	−0.324	1.437
		h(Cu)-t	−1.141	−0.324	1.432
		t-b-t	−1.280	−0.340	1.471
		b	−1.066	−0.267	1.380

contrast to pure Ag_{13} and Cu_{13} nanoparticles, there is no structural change in an $Ag_{12}Cu_1$ bimetallic nanoparticle of core–shell or alloy structures. As mentioned, the energy difference between the COh and Ih structure in an $Ag_{12}Cu_1$ bimetallic nanoparticle is less than that of pure Ag and Cu nanoparticles. We speculate that if the energy difference between isomers is sufficiently small, there will be no structural change because there is no need for the isomers to change their states. An $Ag_{12}Cu_1$ bimetallic nanoparticle has a good renewability.

In our DFT calculations, we considered three adsorption sites for the atomic oxygen; top, bridge, and hollow. The results show that the hollow site is the most stable site. As shown in Fig. 2(b), we optimized the adsorption configuration of two oxygen atoms. The configuration includes an additional oxygen atom that is adsorbed on another hollow site near a pre-adsorbed oxygen atom on the hollow site.

For the O_2 dissociation reaction, we used the three configurations of an adsorbed oxygen molecule as the initial structure and the configuration of two adsorbed oxygen atoms as the final structure. These configurations enabled us to find various reaction pathways, and we calculated the energy barriers by using transition state calculations. Here, too strong or too weak adsorption energy induces a lower ORR activity [32]. If O_2 is strongly adsorbed on a nanoparticle, the reaction rate tends to be decreased. Weak adsorption energy, on the other hand, induces a strong dissociation energy barrier. In our study, the Cu_{13} nanoparticle has the high adsorption energy for an oxygen molecule; it reduces the binding energy between oxygen atoms in the adsorbed oxygen molecule. Our results verify that weak O–O binding energy is represented by the longer bond length in Table 1. As a result, we predict that the Cu_{13} nanoparticle, which has the high adsorption energy, has a low dissociation barrier. In the Ag_{13} nanoparticle, the oxygen molecule is adsorbed in a weak manner. We therefore predict that Ag_{13} has a higher dissociation energy barrier than Cu_{13}. The adsorption energy of the oxygen molecule and the bond length of O–O help us predict the energy barrier of the O_2 dissociation reaction.

Fig. 5 shows the relation between the energy barrier and the adsorption energy of Ih structure. High adsorption energy of reactant is one of the factors to enhance the catalytic performance. O_2 adsorption energy is higher on an Ih $Ag_{12}Cu_1$ (alloy) nanoparticle than on a COh $Ag_{12}Cu_1$ (alloy) nanoparticle. Thus we performed calculations to obtain the energy barrier in O_2 dissociation using Ih nanoparticles. We considered every initial and final configuration for O_2 dissociation. However we reported only the pathway which have smallest energy barrier in each initial configuration. As predicted, the Ag_{13} nanoparticle has the high energy barrier for O_2 dissociation, whereas the Cu_{13} nanoparticle has the low energy barrier. In the case of bimetallic nanoparticles, $Ag_{12}Cu_1$ (alloy) has the slightly lower energy barrier and the higher adsorption energy than $Ag_{12}Cu_1$ (core–shell). The O_2 dissociation is the factor that determines the ORR rate. The low energy barrier increases the ORR rate. The Cu_{13} and $Ag_{12}Cu_1$ (alloy) nanoparticles are good candidates for a catalyst. The Cu_{13} nanoparticle is also good for adsorbing the reactant, O_2. However, its isomers undergo structural change by O_2 adsorption as mentioned. Cu_{13} nanoparticle is poor for the renewability. In addition, the excessively strong adsorption of O_2 on Cu nanoparticles can hinder the subsequent reaction and reduce the

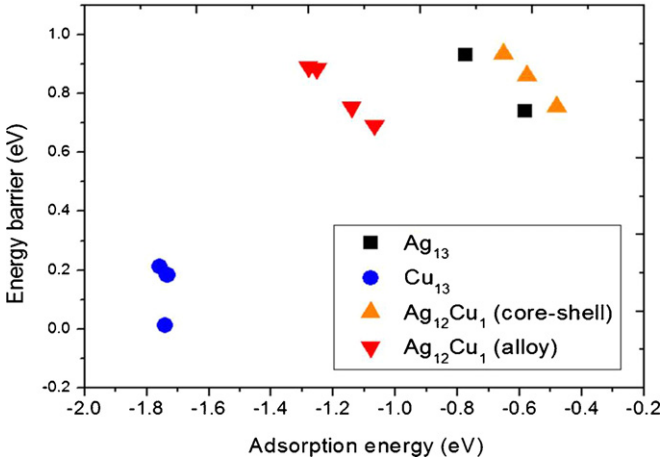

Fig. 5. Relation between the dissociation energy barrier and the adsorption energy for every adsorption sites in the Ih structure of Ag_{13}, Cu_{13}, $Ag_{12}Cu_1$ (core–shell), and $Ag_{12}Cu_1$ (alloy) nanoparticles. The values of lowest energy barrier for Ag_{13}, Cu_{13}, $Ag_{12}Cu_1$ (core–shell), and $Ag_{12}Cu_1$ (alloy) nanoparticles are 0.742 eV, 0.012 eV, 0.756 eV and 0.692 eV, respectively.

overall ORR rate. For the stability of a continuous chemical reaction, $Ag_{12}Cu_1$ (alloy) is better than pure Cu_{13}. Comparing the O_2 adsorption energy and O_2 dissociation energy barrier on $Ag_{12}Cu_1$ (alloy) nanoparticle with those on Pt (1 1 1), $Ag_{12}Cu_1$ (alloy) nanoparticle has stronger O_2 adsorption energy of −1.28 eV than Pt (1 1 1) (−0.34 eV). Although energy barrier of 0.75 eV is relatively higher than 0.38 eV of Pt (1 1 1) [42], it is acceptable when considering the extremely small size of $Ag_{12}Cu_1$ nanoparticle.

4. Conclusion

Our DFT calculations confirm Cu, which has a relatively high surface energy, tends to occupy the core position in an AgCu bimetallic nanoparticle. Therefore, $Ag_{12}Cu_1$ (core–shell) is energetically more stable than $Ag_{12}Cu_1$ (alloy). In an $Ag_{12}Cu_1$ (core–shell) bimetallic nanoparticle, the energy difference between the COh and Ih structures is reduced because the Cu substitution alleviates the stress and strain in the Ih structure.

The O_2 adsorption energy of $Ag_{12}Cu_1$ (alloy) nanoparticle is two times higher than that of Ag_{13} nanoparticle. $Ag_{12}Cu_1$ (core–shell) nanoparticle has no significant benefit for the O_2 adsorption on the surface of the nanoparticle. Additionally, Alloying with Cu prevents any structural transformation and enhances the structural stability during the reaction.

Compared to systems other than Cu_{13}, the $Ag_{12}Cu_1$ (alloy) nanoparticle has the higher adsorption energy for O_2 and a slightly lower energy barrier against O_2 dissociation. In addition, there is no structural change during the ORR. The structural stability and the activity related to the reaction rate are important for a high catalytic performance. Although the $Ag_{12}Cu_1$ (alloy) nanoparticle is more energetically unstable than $Ag_{12}Cu_1$ (core–shell), the alloy nanoparticle can be synthesized provided consideration is given to the composition or kinetic factors. $Ag_{12}Cu_1$ (alloy) appears to be a good candidate for an ORR catalyst.

Acknowledgement

This research was supported by Future-based Technology Development Program (Nano Fields) through the National Research Foundation of Korea (NRF) funded by the Ministry of Education, Science and Technology (2011-0019163).

References

[1] N.M. Markovic, P.N. Ross, CATTECH 4 (2000) 110.
[2] J.K. Norskov, T. Bligaard, J. Rossmeisl, C.H. Christensen, Nat. Chem. 1 (2009) 37.
[3] J. Zhang, K. Sasaki, E. Sutter, R.R. Adzic, Science 315 (2007) 220.
[4] R.R. Adzic, J. Zhang, K. Sasaki, M.B. Vukmirovic, M. Shao, J.X. Wang, A.U. Nilekar, M. Mavrikakis, J.A. Valerio, F. Uribe, Top. Catal. 46 (2007) 249.
[5] Y. Shao-Horn, W.C. Sheng, S. Chen, P.J. Ferreira, E.F. Holby, D. Morgan, Top. Catal. 46 (2007) 285.
[6] M. Haruta, T. Kobayashi, H. Sano, N. Yamada, Chem. Lett. 16 (1987) 405–408.
[7] M. Valden, X. Lai, D.W. Goodman, Science 281 (1998) 1647–1650.
[8] G.C. Bond, D.T. Thomson, Catal. Rev. Sci. Eng. 41 (1999) 319–388.
[9] M.A.P. Dekkers, M.J. Lippits, B.E. Nieuwenhuys, Catal. Today 54 (1999) 381.
[10] S. Carrettin, P. McMorn, P. Johnston, K. Griffin, G.J. Hutchings, Chem. Commun. 696 (2002) 696–697.
[11] S. Schimpf, M. Lucas, C. Mohr, U. Rodemerck, A. BrJckner, J. Radnik, H. Hofmeister, P. Claus, Catal. Today 72 (2002) 63–78.
[12] S. Carrettin, P. McMorn, P. Johnston, K. Griffin, C.J. Kiely, G.A. Attard, G.J. Hutchings, Top. Catal. 27 (2004) 131–136.
[13] R. Meyer, C. Lemire, S. Shaikhutdinov, H.J. Freund, Gold Bull. 37 (2004) 72–133.
[14] A. Abad, P. Concepcion, A. Corma, H. Garcia, Angew. Chem. 117 (2005) 4134-4137; Angew. Chem. Int. Ed. 44 (2005) 4066-4069.
[15] A.C. Gluhoi, N. Bogdanchikova, B.E. Nieuwenhuys, J. Catal. 229 (2005) 154–162.
[16] T.A. Nijhuis, M. Makkee, J.A. Moulijn, B.M. Weckhuysen, Ind. Eng. Chem. Res. 45 (2006) 3447–3459.
[17] C.H. Christensen, B. Jøgensen, J. Rass-Hansen, K. Egeblad, R. Madsen, S.K. Klitgaard, S.M. Hansen, M.R. Hansen, H.C. Andersen, A. Riisager, Angew. Chem. 118 (2006) 4764-4767; Angew. Chem. Int. Ed. 45 (2006) 4648-4651.
[18] R. Burch, Phys. Chem. Chem. Phys. 8 (2006) 5483–5500.
[19] H.Y. Kim, D.H. Kim, J.H. Ryu, H.M. Lee, J. Phys. Chem. C 113 (2009) 15559.
[20] H.Y. Kim, H.G. Kim, D.H. Kim, H.M. Lee, J. Phys. Chem. C 112 (2008) 17138.
[21] H.Y. Kim, H.G. Kim, J.H. Ryu, H.M. Lee, Phys. Rev. B 75 (2007) 212105.
[22] J. Graciani, J. Oviedo, J.F. Sanz, J. Phys. Chem. B 110 (2006) 11600.
[23] N.A. Khan, A. Uhl, S. Shaikhutdinov, H.J. Freund, Surf. Sci. 600 (2006) 1849.
[24] P.A. Sheth, M. Neurock, C.M. Smith, J. Phys. Chem. B 109 (2005) 12449.
[25] F. Studt, F. Abild-Pedersen, T. Bligaard, R.Z. Sorensen, C.H. Christensen, J.K. Norskov, Science 320 (2008) 1320.
[26] F. Studt, F. Abild-Pedersen, T. Bligaard, R.Z. Sorensen, C.H. Christensen, J.K. Norskov, Angew. Chem. 120 (2008) 9439-9442; Angew. Chem. Int. Ed. 47 (2008) 9299-9302.
[27] Y. Gao, N. Shao, S. Bulusu, X.C. Zeng, J. Phys. Chem. C 112 (2008) 8234.
[28] P. Pyykko, N. Runeberg, Angew. Chem. 114 (2002) 2278-2280; Angew. Chem. Int. Ed. 41 (2002) 2174-2176.
[29] Y. Gao, S. Bulusu, X.C. Zeng, J. Am. Chem. Soc. 127 (2005) 15680.
[30] M. Haruta, Catal. Today 36 (1997) 153–166.
[31] B. Hammer, Top. Catal. 37 (2006) 3–16.
[32] J.K. Norskov, J. Rossimeisl, A. Logadottir, L. Lindqvist, J.R. Kitchin, T. Bligaard, H. Jonsson, J. Phys. Chem. B 108 (2004) 17886–17892.
[33] Current Primary and Scrap Metal Price, http://www.metalprices.com/.
[34] F. Baletto, R. Ferrando, Rev. Mod. Phys. 77 (2005) 371–423.
[35] D. Tian, H. Zhang, J. Zhao, Solid State Commun. 144 (2007) 174–179.
[36] Z.Y. Jiang, K.H. Lee, S.T. Li, S.Y. Chu, Phys. Rev. B 73 (2006) 234323.
[37] K. Michalelian, N. Rendoin, I.L. Garzon, Phys. Rev. B 60 (1999) 2000–2010.
[38] C. Mottet, G. Treglia, B. Legrand, Surf. Sci. 383 (1997) L719–L727.
[39] G. Rossi, A. Rapallo, C. Mottet, A. Fortunelli, F. Baletto, R. Ferrando, Phys. Rev. Lett. 93 (2004) 105503.
[40] W.R. Tyson, W.A. Miller, Surf. Sci. 62 (1977) 267–276.
[41] B. Hammer, J.K. Norskov, Adv. Catal. 45 (2000) 71–129.
[42] J.L. Gland, B.A. Sexton, G.B. Fisher, Surf. Sci. 95 (1980) 587–602.